Paper ID: 115

"Numerical Analysis and fabrication of Cupric Oxide-Based Solar Cells"

Fahmida Naznin Ritu[1], Jannatul Mauya[1], A.K.M. Ahsanul Habib[1], Md. Aminul Islam[1]
[1]Department of Materials Science & Engineering, Rajshahi University of Engineering and Technology (RUET), Kazla, Rajshahi 6204
E-mail: fahmidanaznin28@gmail.com, chaity0405@gmail.com, ahsanulhabibsoron@gmail.com, aminul@mse.ruet.ac.bd

Abstract

The optimal band gap, good electron mobility and high minority carrier diffusion length made CuO an ideal candidate to be used as a solar cell absorber layer. In order to better investigate and optimize the performance of CuO-based solar cells, this research was focused on numerical analysis and fabrication of these devices. The main goal of this research was to evaluate the performance of CuO-based solar cells under different operating conditions by using mathematical models and fabricating. In this study, CuO was used as an absorber layer and TiO_2 as ETL, as back contact Cu was used. From this investigation the maximum efficiency was found 19.34% along with Voc 0.8347 V, Jsc 27.49 mA/cm^2 and FF% 83.49%. The optimum absorbing layer thickness and ETL layer thickness were found 5000nm and 200nm respectively. The highest PEC was found at defect density of 10^6 m^{-3} and carrier concentration of 10^{16} cm^{-3}. A CuO based solar cell was also fabricated through spin coating process. From XRD analysis CuO and TiO_2 thin films were confirmed. Band gaps of CuO thin film and TiO_2 thin film were obtained 1.55eV for and 3.2eVrespectively from UV-Visible spectroscopy. Open circuit voltage of 97.9 mV was obtained in the presence of sunlight. This investigation had practical consequences for solar cell device design and optimization that go beyond theoretical comprehension. The performance of the solar cell was optimized through the further numerical investigations of the effect of thickness and carrier concentration of CuO absorber layer. CuO based solar cells offered a cost-effective and sustainable alternative to traditional solar technologies due to the abundance of copper oxide. Their flexibility allowed for innovative applications, and their use aligned with environmental goals, making them a promising area for future development in photovoltaics.

Keywords: Solar Cell, CuO, TiO_2, SCAPS 1D, XRD.

1. Introduction

Modern day silicon-based solar cells has some limitations due to their high manufacturing cost and the limited availability of resources [1]. Copper oxide (CuO), a p-type metal oxide semiconductor, with good conductivity and programmable bandgap offers opportunities for innovative device topologies and enhanced performance [2]. This material has the potentiality to overcome the limitations of silicon-based solar cell due to its low price and abundance. However, CuO-based solar cells have several inherent disadvantages, including limited carrier mobility and stability issues, despite these promising features. Copper oxide (CuO), a black solid stable oxide of copper, has a bandgap of 1.2 eV, monoclinic crystal structure with adsorption coefficient 105 cm^{-1}, the electrical resistivity of about 10 to 105 Ω.cm and high thermal conductivity[1]–[6]. CuO material has numerous other benefits also, including montoxicity, comparatively simple preparation process, and individual square planar coordination of copper and oxygen [4]. CuO is widely utilized as an active layer in some kinds of photovoltaic structures[1], [5], [6] . SCAPS has a user-friendly interface where one can provide the known parameters of a material and make an individual layer. At the same place all the other layers can be created, and the solar cell can be simulated to find the efficiency. The highest power conversion efficiency of solar cells based on the CuO material can be obtained up to 23.82% [7]. As researchers deeply investigating the complexity of CuO-based solar cell technology, this article investigated different parameters effect such as, temperature effect, layers thickness effect, doping effect, QE etc on CuO based solar cell. Photovoltaic (PV) solar systems are constructed and modeled using solar simulation software. The thin-film planar FTO/TiO2/CuO solar cell's J–V, C–V, and QE photovoltaic properties were simulated using SCAPS (version 3.3.07). These features served as the basis for the calculation and analysis of the most crucial metrics, including power conversion efficiency (η), fill factor (FF), open circuit voltage (V_{oc}), and short circuit current density (J_{sc}) under standard illumination (AM 1.5 G, 100 mW cm−2, 300 K). Table 1 shows the summary of the simulation work on CuO based solar cell.

Table 1: CuO based solar cell

Configuration	Voc (V)	Jsc (mA/cm^2)	FF%	PCE%	References
FTO/CuO/IGZO	0.8408	27.32	85.1	19.6	[3]
FTO/CuO/WS_2	0.8508	27.38	85.3	19.5	[4]
FTO/CuO/CdS	0.8516	27.26	83.9	19.2	[4]
FTO/TiO_2/CuO	0.84	27.74	84.83	19.42	[5]
FTO/CuO/CdS	0.949	28.48	87.27	16.37	[7]

FTO/CuO/ZnO	1.2353	2.74	0.787	20.13	[8]
FTO/CuO/ZnO/Cu_2O	0.8344	28.44	81.83	19.13	[9]

The literature provided the characteristics of the materials utilized in the simulations. Table 2 provides the parameters utilized in the simulations for FTO, TiO_2, and CuO. The thin-film planar FTO/TiO2/CuO heterojunction solar cell's optimized structure served as the foundation for an investigation of the cell's performance at various operating temperatures and sunlight concentrations. Fig. 1 is showing the band gap diagram and cell structure of the CuO based solar cell.

Table 2: Device parameters of simulated solar cell

Parameters	CuO [9]	TiO_2 [10]	FTO [11]
Thickness (nm)	2000	2000	800
Band gap (eV)	1.5	3.2	3.5
Electron affinity (eV)	4.3	4.2	4.2
Dielectric permittivity (relative)	18.1	10	14.5
CB effective density of states (cm^{-3})	$2.2x10^{19}$	$2.2x10^{17}$	$2x10^{18}$
VB effective density of states (cm^{-3})	$5.5x10^{20}$	$6x10^{17}$	$1.8x10^{19}$
Electron thermal velocity (cm/s)	$1x10^{7}$	$1x10^{7}$	$1x10^{7}$
Hole thermal velocity (cm/s)	$1x10^{7}$	$1x10^{7}$	$1x10^{7}$
Electron mobility (cm^2 /V s)	100	100	$2x10^{1}$
Hole mobility (cm^2 /V s)	0.1	250	$1x10^{1}$
Shallow uniform donor density N_D (cm^{-3})	0	10^{17}	0
Shallow uniform acceptor density N_A (cm^{-3})	10^{16}	0	$2x10^{19}$
Absorber Defect (cm^{-3})	10^{11}	10^{11}	10^{11}
Interface Defect (cm^{-3})	10^{11}	10^{11}	10^{11}
Defect type at bulk/interface Donor/Neutral	Neutral	Neutral	Neutral

2.Methodology

2.1 Simulation

The SCAPS-1D simulator uses the solutions of the Poisson's equation (Eq. 1), the electron continuity equation (Eq. 2), and the hole continuity equation (Eq. 3) for simulating semiconductor devices. SCAPS-1D software analyzes these three associated partial differential equations to determine the current density (Jsc), quantum efficiency (QE), energy band, and current–voltage characteristics.

$$-\frac{\partial}{\partial x}\left(-\varepsilon(x)\frac{\partial V}{\partial x}\right) = q\left[p(x) - n(x) + N^{+}_{D}(x) - N^{-}_{A}(x) + p_t(x) - n_t(x)\right] \quad (1)$$

$$\frac{\partial n}{\partial t} = \frac{1}{q}\frac{\partial Jn}{\partial x} + G_n - R_n \quad (2)$$

$$\frac{\partial p}{\partial t} = = \frac{1}{q}\frac{\partial Jp}{\partial x} + G_p - R_p \quad (3)$$

Here, q = Charge, ε = Dielectric permittivity, V = Potential, p(x) = Free holes concentration, n(x) = Free electrons concentration, $N^{+}_{D}(x)$ = Ionized donor concentration, $N^{-}_{A}(x)$ = Ionized acceptor concentration, $p_t(x)$ = Trap density of hole, $n_t(x)$ = Trap density of electron, J_n = Current density of electron, J_p = Current density of holes, G_n = Rate of electrons generation, G_p = Rate of holes generation, R_n = Recombination rate of electron, R_p = Recombination rate of hole.

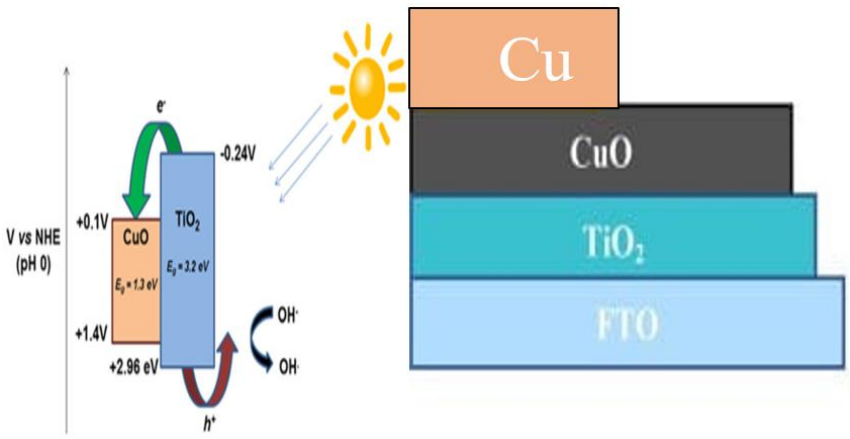


Figure 1: Band gap diagram and cell structure of CuO based solar.

2.2 Experimental procedure

2.2.1 FTO/TiO2/CuO thin film preparation

Commercially available TiO_2 powder were used to prepare TiO_2 thin film on a Flourine Doped Tin Oxide (FTO) substrate using spin coater. Then the sol-gel process involves the deposition of a precursor solution of cupric acetate, sodium acetate and isopropyl alcohol on FTO/TiO_2 coated glass substrate using Spin coater, followed by

heat treatment at 450°C for 1 hour to convert it into FTO/TiO_2/CuO thin film. After the junction formation Cu wire was used to establish electrical connections. Prior to the preparation of CuO thin film, the glass substrate and the Flourine Doped Tin Oxide (FTO) coated glass substrate used were cut and ultrasonically cleaned with acetone, methanol, iso-propanol, and kept in staining jar and allow to dry in vacuum oven. The prepared sample was characterized with X-ray Diffraction (XRD) and UV-Visible Spectroscopy (UV-Vis) to reveal structural and optical properties respectively.

3. Results and discussions

The solar cells output is highly dependent on its operating temperature. Here, Fig. 2 is showing the calculation of the temperature dependence of PV performance matrices. The overall performance is optimal at 250K according to Fig. 3 which showing the temperature effect on I-V curve. The values at optimal point are Voc of 0.9490 V, Jsc of 27.62 mA/cm^2 and FF of 84.97%. Khattak et al. [12] also got similar result in their work energy gap value of 1.53 eV and thickness of 292 nm produces the highest efficiency of 13.38%, Voc = 0.94 V, Jsc = 17.31 cmA cm−2 and FF = 81.47%. The increasing trend of J_{SC} took place due to the thermal generation of carriers [11], [13].

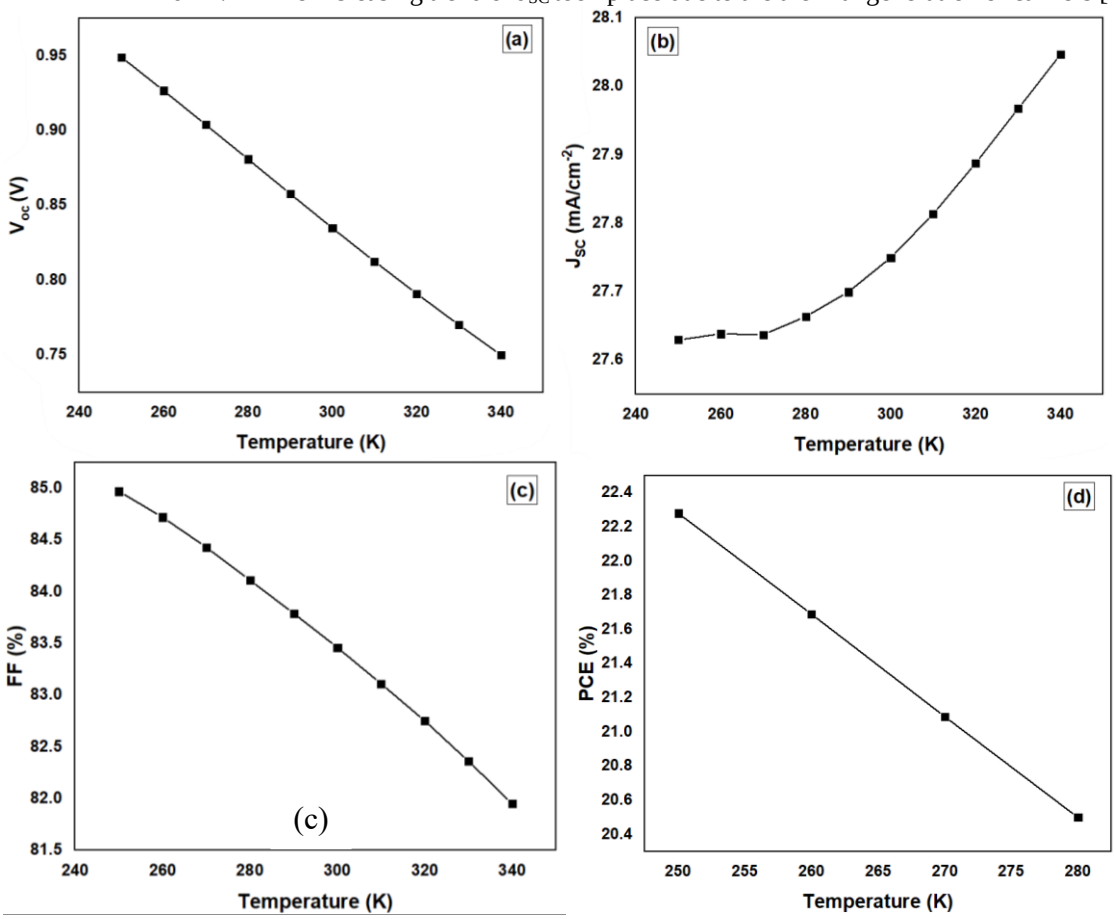


Figure 2: Effect of temperature on (a) Voc, (b)Jsc, (c) FF% and (d) PCE%.

The absorber layer thickness has also a strong impact on solar cell performance. Fig. 4 is showing the calculation of the absorbing layer thickness dependence of PV performance matrices. According to Fig. 5 the thickness around 2000 nm is significant for all the devices. The PCE value fell from 20.34% (5000 nm) to 19.44% (9000 nm), Voc increased from 0.82 to 0.84 V, Jsc increased from 25.93 to 28.69 mA/cm^2 and FF increased from80.23% to 80.7%. Sawicka-Chudy et al. [6] found the variation of the CuO absorber layer's thickness, ranging from 0.1 µm to 1 µm, with the band gap energy set at 1.53 eV, while holding the remaining parameters constant got similar result. The thickness of ETL is crucial for obtaining optimal performance. The thickness of ETL is altered from 200nm to 3200nm. Fig. 6 shows that Voc and FF% remain almost constant whereas a slight decreased in Jsc and PCE 2000 are observed. Therefore, the ETL thickness of 200 nm is chosen as optima. The interface defects have much more impact on efficiency of the solar cell at moderate values as well. The interface defect reduces the efficiency drastically for CuO/TiO_2 solar cell which is shown in Fig. 7. The proposed structures with optimized parameters resulted in enhanced performance, with structures seeing an improved efficiency of up to 19.34% of interface defect 10^6. In a solar cell, recombination acts to restore the non-equilibrium light generated electron hole pair (EHP) population to its thermal equilibrium value. The three types of recombination in a bulk semiconductor are: radioactive, non-radioactive and auger recombination. In this study, Fig. 8 shows that the efficiency decreases

with radioactive recombination co-efficient increases. The PCE is optimal at radioactive recombination co-efficient of 10^{-15}. CuO is an intrinsic p-type material where the carrier concentration depends on the defects and stoichiometry of the synthesized material. The carrier concentration of the absorber layer is varied in the range of 10^{0} -10^{24}cm^{-3}. It can be observed from the Fig.9 which shows that the efficiency starts increasing with increase in the concentration. In this study, carrier concentration of 10^{16} cm^{-3}, the PCE is optimal. Additionally, the increase in carrier concentration reduces the depletion width in absorber layer which has impact on separation of photo generated charges which leads to reduction in short circuit current. Senthikumar et al. [9] observed simila result in their work. Fig. 10 displays the contour plot analysis of CuO/TiO_2 solar cells were simulated as a function of shallow uniform donor density N_D for the CuO structure. The N_D values varied in the range from 10^3 cm^{-3} to 10^{16} cm^{-3} with constant N_A=10^{17} 1/cm^3 for TiO_2. The contour plot shows that, PCE decreases with shallow uniform

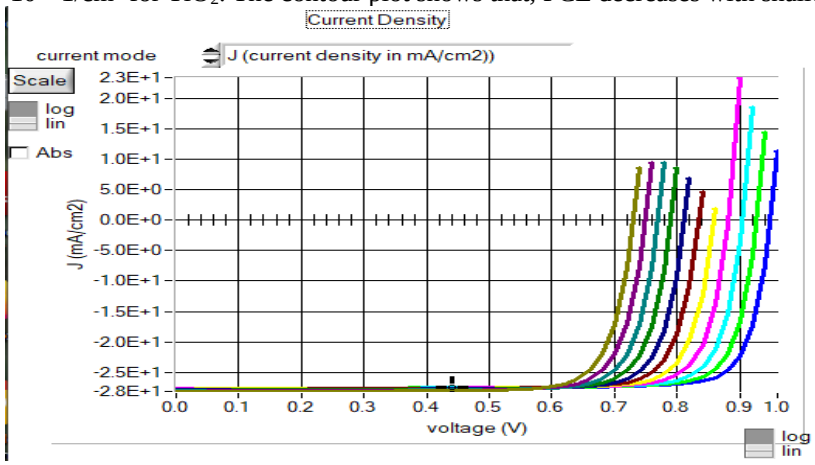


Figure 3: Temperature effect on I-V curve.

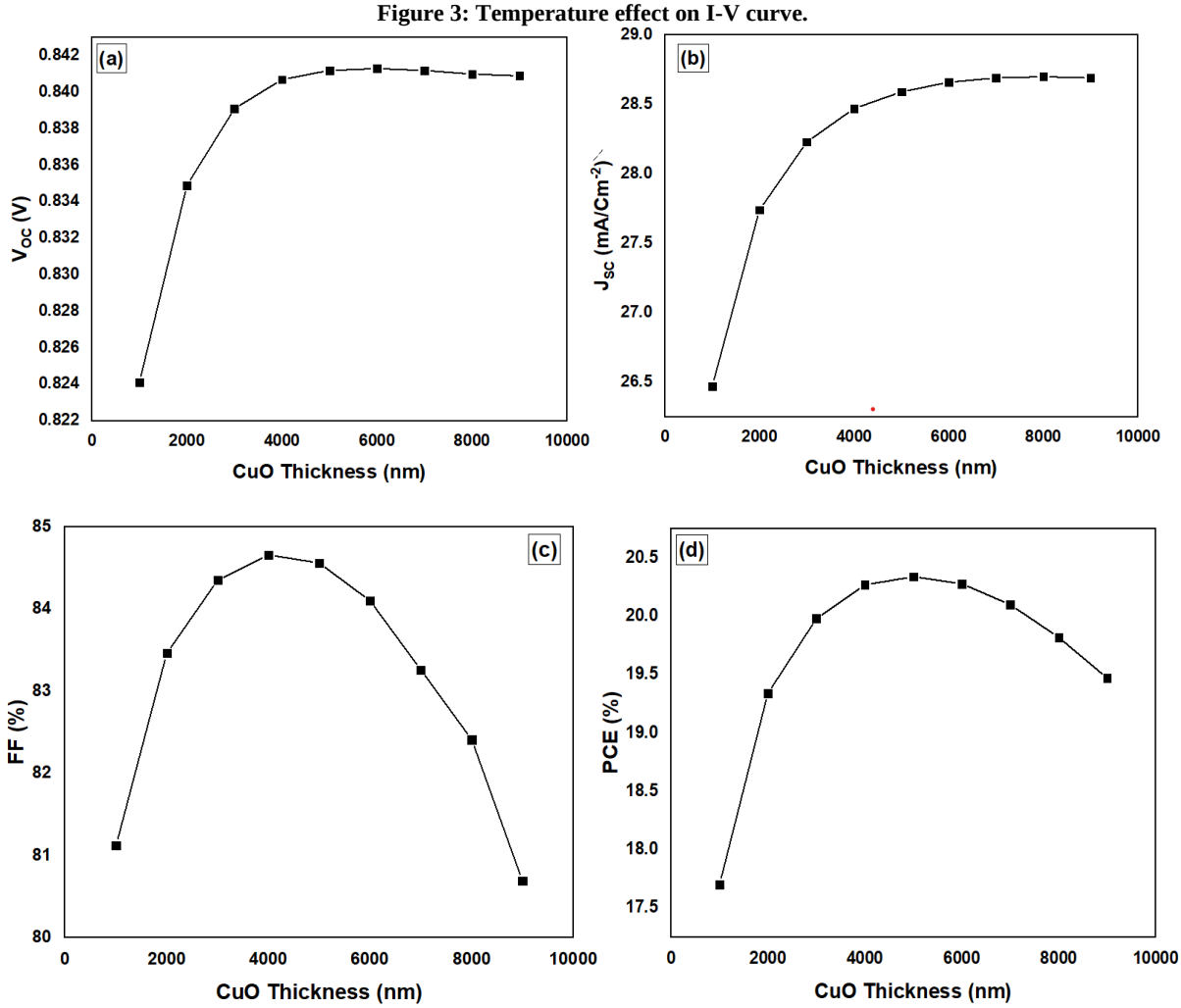


Figure 4: Effect of absorbing layer thickness on (a) Voc, (b)Jsc, (c) FF% and (d) PCE%.

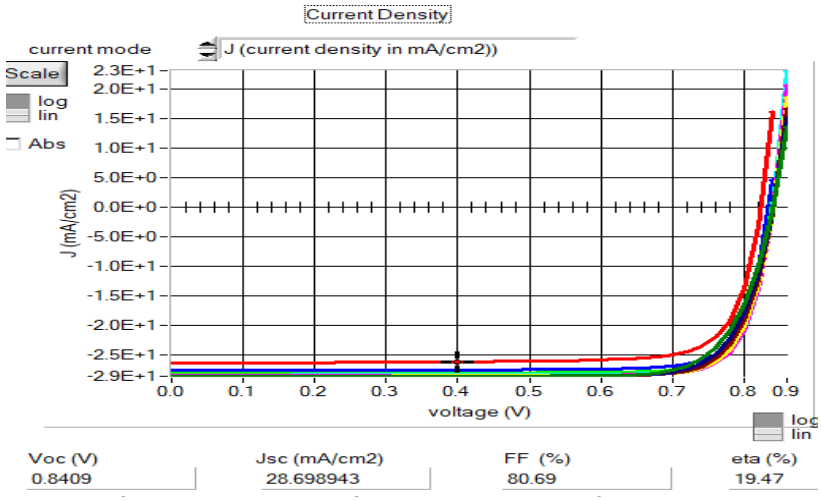


Figure 5: Absorbing layer thickness effect on I-V curve.

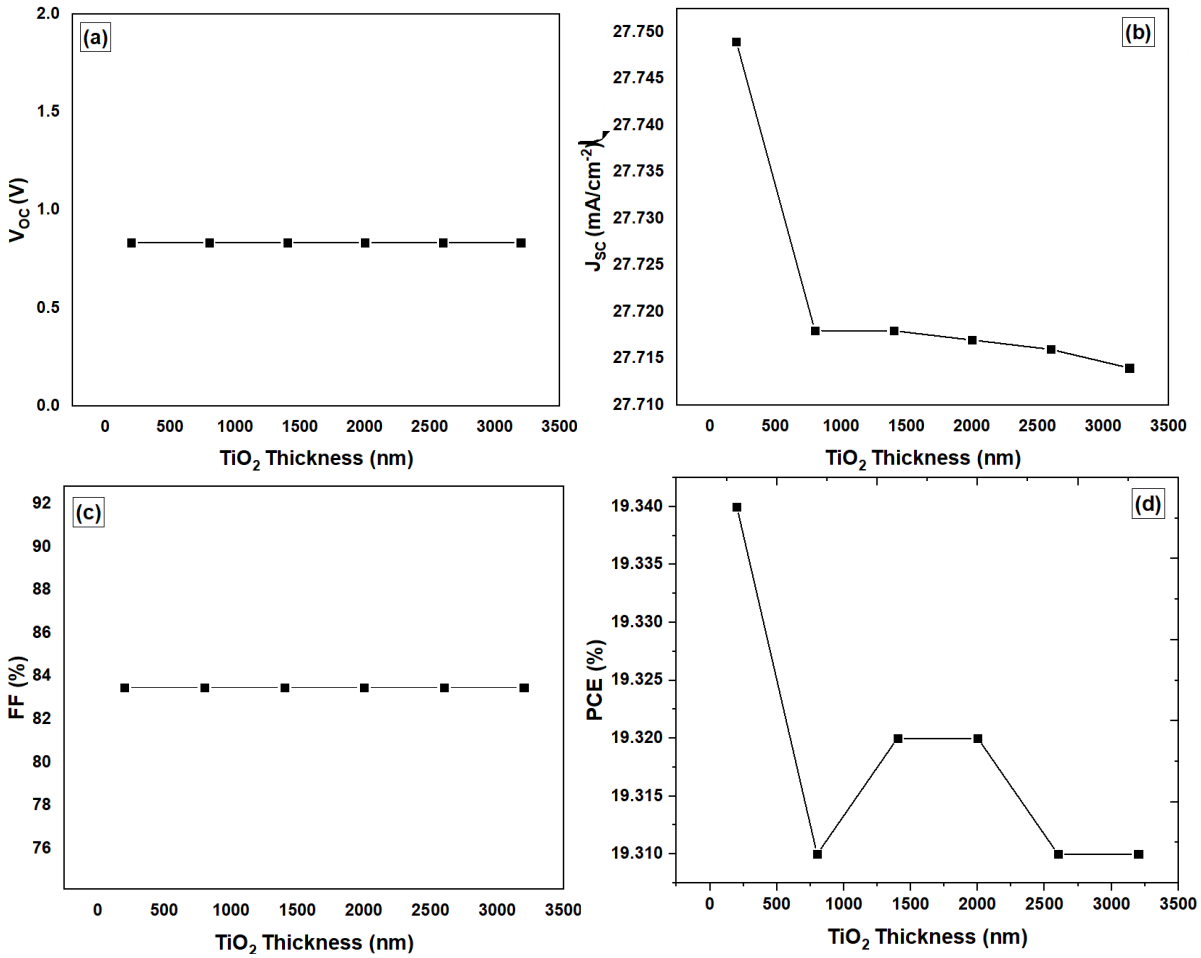


Figure 6: Effect of ETL layer thickness on (a) Voc, (b)Jsc, (c) FF% and (d) PCE%.

donor density at a thickness of 0.5 µm. But we have found optimal PCE at a thickness of 3 µm with 10^{16} cm^{-3} shallow uniform donor density. Abdelkarim et al. [11] found the Voc value was nearly no change as the shallow donor density increases up to 10^{18} cm^{-3} and dropped as the higher shallow donor density. Therefore, in that work, the optimized shallow donor density was 10^{17} cm^{-3}. Fig. 11 displays the contour plot analysis of CuO/TiO_2 solar cells were simulated as a function of shallow uniform acceptor density N_A for the CuO structure. The N_A values

varied in the range from 10^3 cm^{-3} to 10^{16} cm^{-3} with constant $N_D=10^{17}$ cm^{-3} for TiO_2. The contour plot shows that, PCE increases with shallow uniform acceptor density and thickness. At a thickness of 2.5 μm with 10^{15} $1/cm^3$ acceptor density, the efficiency is 19.72%. The optimal PCE at a thickness of 3micrometres with 10^{16} cm^{-3} shallow uniform acceptor density and it is 19.98%. Fig. 12 shows the efficiency of the solar cell initially increases with longer wavelengths, reaches a peak, and then declines. This behavior occurs because the material's response

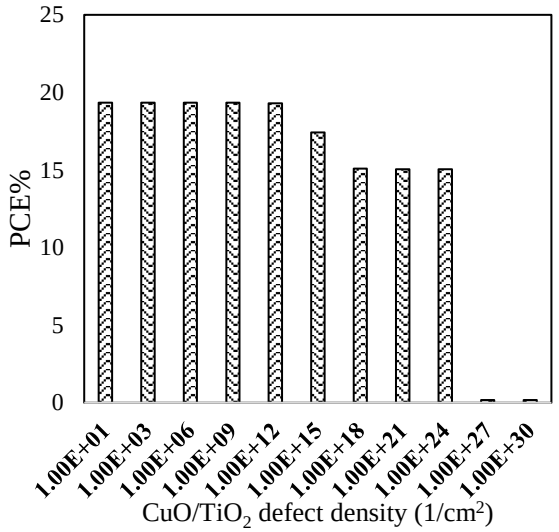


Figure 7: Effect of interface defect density on PCE%.

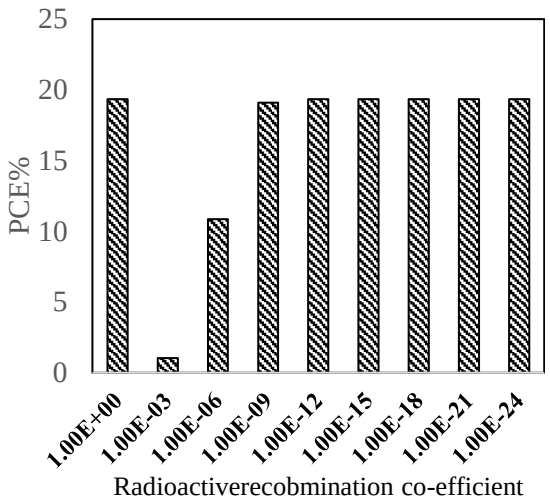


Figure 8: Effect of radioactive recombination on PCE%.

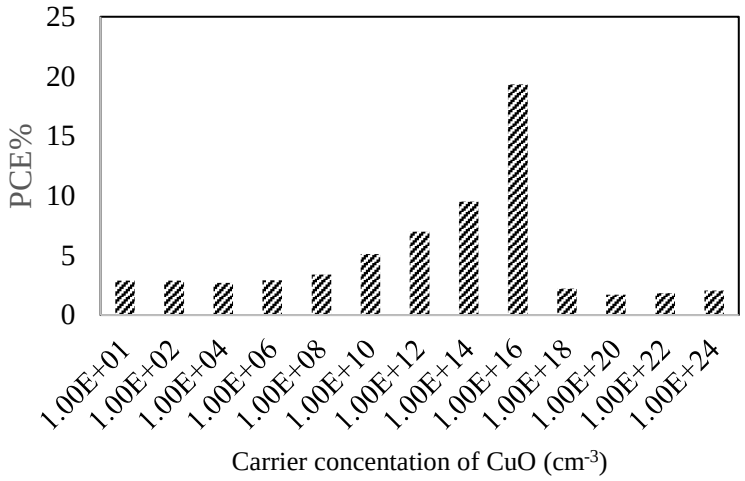


Figure 9: Effect of carrier concentration.

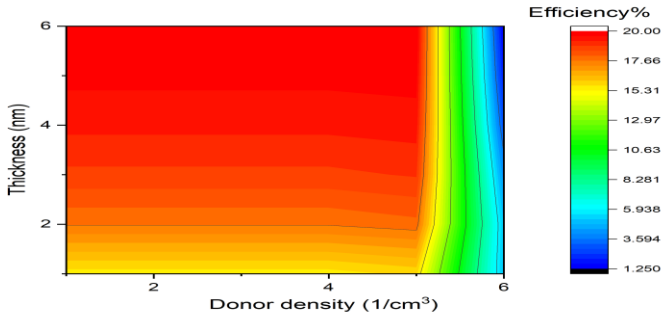


Figure 10: Shallow uniform donor density variation of absorber layer with thickness and efficiency.

to different wavelengths relies on its quantum properties. As a result, if the wavelength is either too short or too long, the efficiency falls. Solar rays with wavelengths ranging from 300 to 900 nm is often adequate to liberate electrons from their weak bonds and create an electric current. This phenomenon is linked to the band gap of the

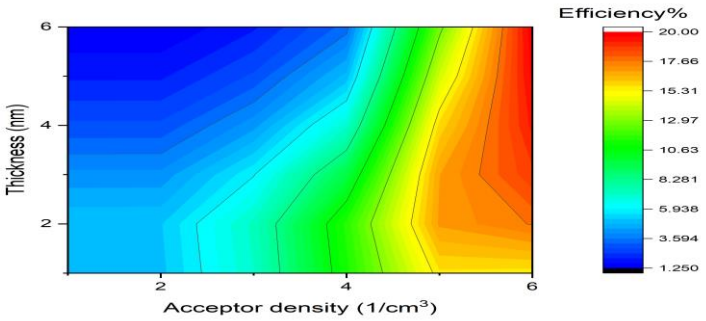


Figure 11: Shallow acceptor density variation of absorber layer with thickness and efficiency.

material. Photos with energies over the band gap are absorbed but create extra energy loss as heat, whereas photons below the band gap are not absorbed. Yet due to quantum effects in the material, the precise range may vary. The highest efficiency is attained at a wavelength of 360 nm in this simulation.

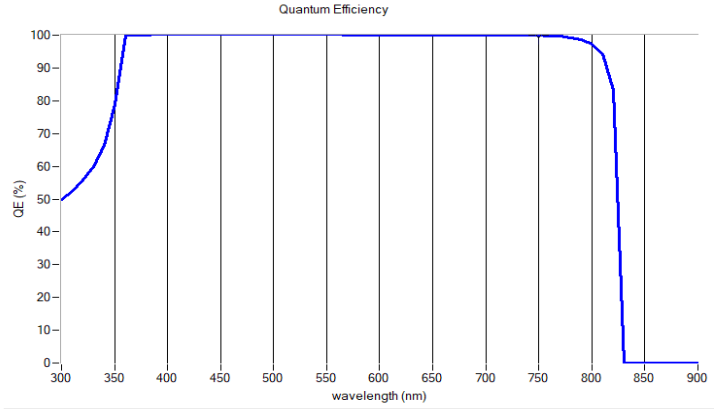


Figure 12: Analysis of QE (%).

XRD was performed to confirm the successful synthesis of CuO and TiO_2 thin film. From Fig. 13 it is observed that the characterization peak of TiO_2 is observed for (120), (210) and (211) which well matched with JCPDS No. 00-053-0619 and confirms the successful synthesis of TiO_2 thin film. Again, for CuO characterization peak observed for (110), (111), (200), (211), and (311) which well matched with JCPDS No.00-005-0667 and confirms the successful synthesis of CuO thin film. Therefore, XRD confirms the existence of both layers which forms junctions for the solar cell.

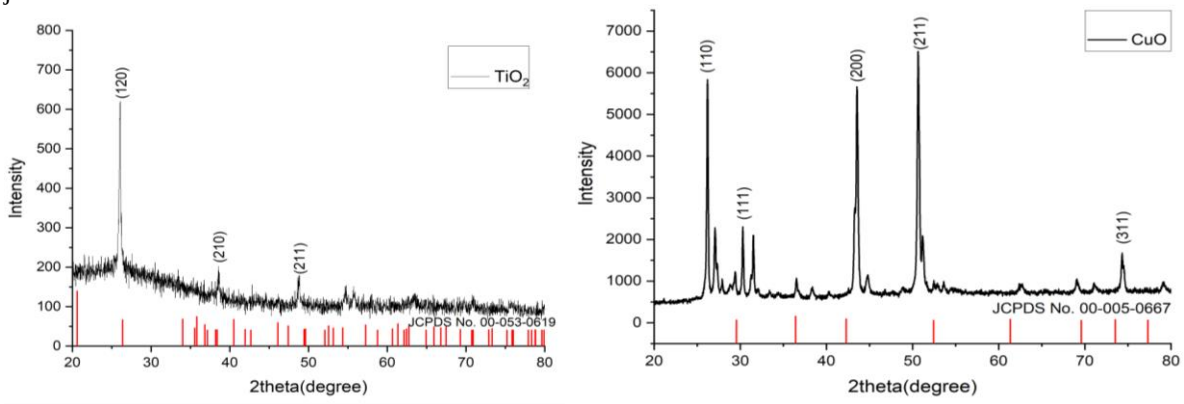


Figure 13: XRD peak position of TiO_2 and CuO thin film.

UV-Vis spectroscopy was conducted for both TiO_2 and CuO sample to observe its optical absorption and band gap energy. The absorption is continuously decreased when the wavelength increases due to lower energy. The Tauc plotting was used to determine the bandgap of the thin films. The band was for 3.2 eV and 1.51 eV for TiO_2 and CuO respectively.

Table 3: Result from simulation

Configuration	Voc (V)	Jsc (mA/cm^2)	FF%	PCE%
CuO/TiO_2/FTO	0.8349	27.749640	83.46	19.34

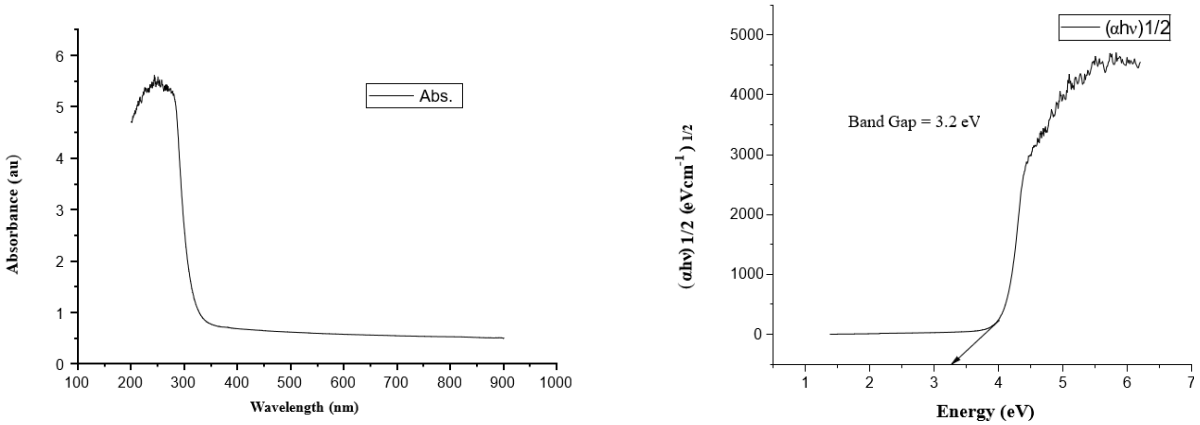


Figure 14: UV-Vis analysis and Tauc plot of TiO_2 thin film.

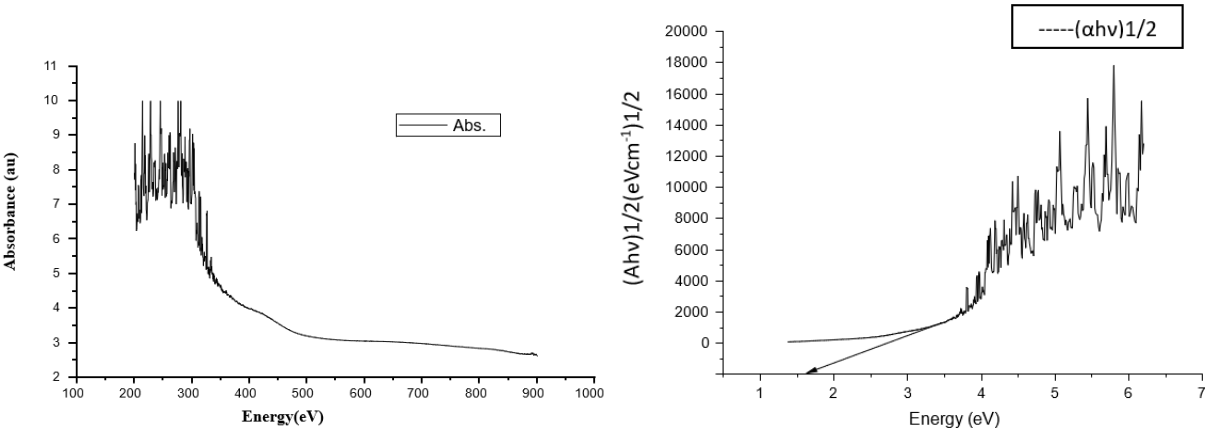


Figure 15: UV- vis analysis of CuO thin film.

Table 4: Comparison between our findings and literature

Our findings	Literature
Configuration: CuO/TiO_2/FTO	Configuration: CuO/TiO_2/FTO
Result (simulation) : PCE 19.34%	Result (simulation): PCE 19.42% (G. Shukla, P.K. Mishra, A. Khare, J. Alloys Compd. 489 (2010) 246–251)

4.Conclusions

SCAPS-1D was used to mimic the performance of CuO/TiO2 thin-film solar cells. Our research showed that a CuO layer works better in solar cells as an absorber layer. Many PV factors were found to have I-V characteristics, and the application of CuO/TiO2 solar cells was investigated through parameter analysis that may have contributed to the efficiency gain. The results of the numerical study showed a high efficiency of 19.34%. The PCE is ideal for the absorbing layer at a thickness of 5000 nm, at 106 PCE for carrier concentration, and at 10-5 radioactive recombination coefficient is highest. After optimization of each layer a noteworthy open circuit current density of 0.8349 mA/cm^2, short circuit current density of 27.749640 mA/cm^2 and FF 83.46% are achieved. In the presence of sunlight, voltage was measured 97.9mV.

References

[1] S. Hussain *et al.*, "Fabrication and photovoltaic characteristics of Cu2O/TiO2 thin film heterojunction solar cell," *Thin Solid Films*, vol. 522, pp. 430–434, Nov. 2012, doi: 10.1016/J.TSF.2012.08.013.

[2] K. Mageshwari and R. Sathyamoorthy, "Physical properties of nanocrystalline CuO thin films prepared by the SILAR method," *Mater. Sci. Semicond. Process.*, vol. 16, no. 2, pp. 337–343, Apr. 2013, doi: 10.1016/J.MSSP.2012.09.016.

[3] A. Moumen, B. Hartiti, P. Thevenin, and M. Siadat, “Synthesis and characterization of CuO thin films grown by chemical spray pyrolysis,” *Opt. Quantum Electron.*, vol. 49, no. 2, Feb. 2017, doi: 10.1007/S11082-017-0910-1.

[4] G. Enebe, K. Ukoba, T. J.-A. Energy, and undefined 2019, “Numerical modeling of effect of annealing on nanostructured CuO/TiO2 pn heterojunction solar cells using SCAPSQ3AIMS Energy; H-Index: 15SJR: Q3 CORE: NA ABDC: NA FT50: NA,” *ujcontent.uj.ac.zaGC Enebe, K Ukoba, TC JenAIMS Energy, 2019•ujcontent.uj.ac.za*, Accessed: Nov. 19, 2024. [Online]. Available: https://ujcontent.uj.ac.za/view/pdfCoverPage?instCode=27UOJ_INST&filePid=135786700007691&download=true.

[5] P. Sawicka-Chudy *et al.*, “Simulation of TiO2/CuO solar cells with SCAPS-1D software,” *Mater. Res. Express*, vol. 6, no. 8, p. 085918, Jun. 2019, doi: 10.1088/2053-1591/AB22AA.

[6] P. Sawicka-Chudy, M. Sibiński, G. Wisz, E. Rybak-Wilusz, and M. Cholewa, “Numerical analysis and optimization of Cu2O/TiO2, CuO/TiO2, heterojunction solar cells using SCAPS,” *J. Phys. Conf. Ser.*, vol. 1033, no. 1, p. 012002, May 2018, doi: 10.1088/1742-6596/1033/1/012002.

[7] Y. Liu, Y. Sun, and A. Rockett, “A new simulation software of solar cells—wxAMPS,” *Sol. Energy Mater. Sol. Cells*, vol. 98, pp. 124–128, Mar. 2012, doi: 10.1016/J.SOLMAT.2011.10.010.

[8] T. Garmim *et al.*, “Synthesis and optimization of SnS absorber layer by spin-coating process and Taguchi approach,” *Mater. Chem. Phys.*, vol. 292, p. 126774, Dec. 2022, doi: 10.1016/J.MATCHEMPHYS.2022.126774.

[9] V. Senthilkumar and P. Vickraman, “Annealing temperature dependent on structural, optical and electrical properties of indium oxide thin films deposited by electron beam evaporation method,” *Curr. Appl. Phys.*, vol. 10, no. 3, pp. 880–885, May 2010, doi: 10.1016/J.CAP.2009.10.014.

[10] Z. Essalhi, B. Hartiti, A. Lfakir, B. Mari, and P. Thevenin, “Optoelectronics properties of TiO2:Cu thin films obtained by sol gel method,” *Opt. Quantum Electron.*, vol. 49, no. 9, Sep. 2017, doi: 10.1007/S11082-017-1142-0.

[11] A. Abdelkrim, S. Rahmane, K. Nabila, A. Hafida, and O. Abdelouahab, “Polycrystalline SnO2 thin films grown at different substrate temperature by pneumatic spray,” *J. Mater. Sci. Mater. Electron.*, vol. 28, no. 6, pp. 4772–4779, Mar. 2017, doi: 10.1007/S10854-016-6122-9.

[12] Y. H. Khattak, F. Baig, S. Ullah, B. Marí, S. Beg, and H. Ullah, “Enhancement of the conversion efficiency of thin film kesterite solar cell,” *J. Renew. Sustain. Energy*, vol. 10, no. 3, May 2018, doi: 10.1063/1.5023478/285554.

[13] A. D. Dhass, Y. Prakash, and K. C. Ramya, “Effect of temperature on internal parameters of solar cell,” *Mater. Today Proc.*, vol. 33, pp. 732–735, Jan. 2020, doi: 10.1016/J.MATPR.2020.06.079.